Cell Death and Differentiation (2011) 18, 996–1004

www.nature.com/cdd

Caspase-3-mediated degradation of condensin Cap-H regulates mitotic cell death

S-K Lai[1,2], C-H Wong[1,2], Y-P Lee[1] and H-Y Li*[,1]

Mitotic death is a major form of cell death in cancer cells that have been treated with chemotherapeutic drugs. However, the mechanisms underlying this form of cell death is poorly understood. Here, we report that the loss of chromosome integrity is an important determinant of mitotic death. During prolonged mitotic arrest, caspase-3 is activated and it cleaves Cap-H, a subunit of condensin I. The depletion of Cap-H results in the loss of condensin I complex at the chromosomes, thus affecting the integrity of the chromosomes. Consequently, DNA fragmentation by caspase-activated DNase is facilitated, thus driving the cell towards mitotic death. By expressing a caspase-resistant form of Cap-H, mitotic death is abrogated and the cells are able to reenter interphase after a long mitotic delay. Taken together, we provide new insights into the molecular events that occur during mitotic death.
Cell Death and Differentiation (2011) **18,** 996–1004; doi:10.1038/cdd.2010.165; published online 10 December 2010

Cellular death has a critical role in cancer progression and treatment. For decades, apoptosis is thought to be the main anti-proliferative response of tumors to anti-cancer therapy.[1–3] However, defects in the apoptotic pathway coupled with mutations in the tumor suppressor p53 gene observed in many tumor types may render the therapy ineffective. It is now increasingly recognized that tumor cells can be induced to die by other non-apoptotic mechanisms such as autophagy, senescence and mitotic catastrophe.[4–7]

The mitotic stage of the cell cycle is a good target in cancer treatments. As tumor cells divide uncontrollably, they pass through a stage that is highly vulnerable to anti-mitotic drugs more frequently compared with normal cells. Therefore, many anti-mitotic drugs, especially microtubule-targeted agents have shown considerable success in killing tumor cells by triggering mitotic death following a prolonged mitotic arrest.[8–10] Despite that, the mechanisms that regulate this form of cell death are poorly understood and little is known about the signaling events that activate the death machinery after a sustained mitotic delay. Furthermore, tumor cells can adopt other cell fates besides death during mitosis.[11,12] The cells can exit mitosis with or without division and reenter interphase. It remains unclear why cells adopt different fates in response to drug treatment, though much research has been done to investigate this phenomenon.[13–15] It is most ideal if the tumor cells die during mitosis instead of exiting mitosis as that will lead to aneuploidy and genetic instability. Thus, it is crucial to decipher the link between mitotic arrest and cell death and elucidate the molecular events that dictate the lethal fate of cells in mitosis.

At present, mitotic death is regarded as a form of cell death that occurs after failed mitosis with apoptotic or necrotic-like features. Caspases, which are known to be the executors of apoptosis in interphase cells,[16] may or may not be involved during mitotic death.[13,17–22] It is noted that although caspases are activated, mitotic death may not be regarded as a classical form of apoptosis as the cellular structure and protein profiles of interphase and mitotic cells are considerably different.

Here, we report a mechanism that links prolonged mitotic arrest, caspase activation and the death machinery. We have found that caspases are activated during prolonged mitotic arrest. Activated caspase-3 cleaves condensin I subunit Cap-H, which leads to a loss of condensin I complex at the chromosomes. As such, chromosomal integrity is altered; making them susceptible to DNA fragmentation by caspase-activated Dnase (CAD). Consequently, the cell is committed to die in mitosis in order to protect it against further genetic alterations.

Results

The mitotic chromosomal integrity is altered as cells undergo mitotic death. To study mitotic death, two anti-mitotic drugs, taxol and vinblastine were used. These drugs suppress the dynamics of spindle microtubules and affect spindle function by stabilizing and depolymerizing microtubules, respectively.[23,24] Timelapse imaging was first carried out to ensure that 10 nM taxol and vinblastine were able to induce mitotic death in HeLa cells. We observed that cells began to arrest in mitosis ~8–12 h after drug addition and majority of the cells died in mitosis after a prolonged arrest (Supplementary Figure S1a). This datum confirmed that both drugs used in this study can effectively induce mitotic death.

[1]Division of Molecular and Cell Biology, School of Biological Sciences, College of Science, Nanyang Technological University, Singapore, Singapore
*Corresponding author: H-Y Li, PhD, Division of Molecular and Cell Biology, School of Biological Sciences, Nanyang Technological University, Singapore 637551, Singapore. Tel: +65 6316 2931; Fax: +65 6791 3856; E-mail: hyli@ntu.edu.sg
[2]These authors contributed equally to this work.
Keywords: mitotic cell death; caspase; condensin
Abbreviations: CAD, caspase-activated DNase; EGFP, enhanced green fluorescent protein; FACS, Fluorescence-activated cell sorting; ICAD, inhibitor of CAD; SEM, scanning electron microscopy; SMC, structural maintenance of chromosome
Received 29.4.10; revised 01.10.10; accepted 10.11.10; Edited by G Salvesen; published online 10.12.10

Maintenance of chromosomal integrity is extremely crucial during mitosis. Any alteration that compromises the integrity of chromosome will lead to reduction in cell viability and eventually cell death.[25,26] We first observed the consequences of prolonged mitotic arrest on the integrity of mitotic chromosomes. Metaphase chromosome spreads from control and drug-treated cells were prepared. Cells were collected 24 h after drug addition by mechanical shake-off in order to enrich the population of prolonged mitosis-arrested cells. We found that sustained mitotic arrest results in longitudinal shortening and widening of the chromosomes (Figure 1a). The length and width of chromosomes were measured and the differences in these two variables between control and drug-treated samples were statistically significant at the $P<0.001$ level (Figure 1b). Measurements of the chromosomes are summarized in Table 1. Additionally, we concluded that the alteration in chromosome morphology only occurs after a long arrest in mitosis because chromosomes from early mitosis-arrested cells showed no obvious modifications (Supplementary Figure S1b) and the Student *t*-test analysis revealed that any differences between control and early mitosis-arrested samples were statistically insignificant. Similar change in chromosome morphology was also observed in taxol-treated A549 cells (Supplementary Figure S2a).

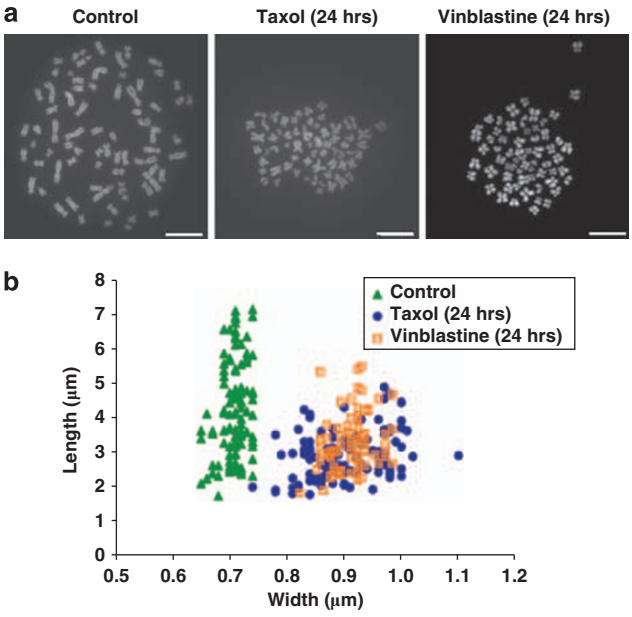

Figure 1 Chromosomal integrity is altered in prolonged mitosis-arrested cells. (**a**) Chromosome spreads of control metaphase cells and mitosis-arrested cells obtained from mechanical shake-off 24 h after taxol or vinblastine addition. (**b**) Width and length of the chromosomes were measured. Differences in these two variables between control and drug-treated cells are statistically significant at $P<0.001$ level. At least 100 chromosomes in a spread were analyzed. Bar, 10 μm

The chromosomes were next analyzed by scanning electron microscopy (SEM) in order to obtain a highly magnified view of the chromosomes. SEM images revealed that chromosomes from control metaphase cells consisted of chromatin fibers that are organized in loops and coils to form a very tight and compact structure. On the contrary, chromosomes from cells that have undergone a prolonged mitotic arrest displayed surface abnormalities. The DNA was clearly less packed with more spaces between the DNA loops. Furthermore, abnormal chromatin protrusions were detected on the chromosome surface. Analysis of at least 50 chromosomes from each sample revealed that 82 and 92% of the chromosomes from taxol and vinblastine-treated cells, respectively, displayed chromosomal abnormalites as described above as compared with 6% from the control cells (Supplementary Figure S1c). These observations further demonstrate that chromosomal integrity is altered during prolonged mitotic arrest.

The loss of chromosomal integrity facilitates DNA fragmentation during mitotic death. DNA breakage is commonly found in mammalian cells that have undergone sustained mitotic arrest.[27,28] As the DNA repair machinery is inefficient during mitosis probably because of the condensed nature of the chromosomes, these breaks often result in reduced cell viability or cell death.[29,30] Presence of any DNA damage was investigated by TUNEL assay. Early and late mitosis-arrested cells were collected 12 and 24 h after drug treatment, respectively. TUNEL labeling was carried out on mitotic cells as well as on individual chromosomes. Positive TUNEL labeling was only observed in cells that have been treated with drug for 24 h, which indicates presence of DNA damage. In contrast, both control mitotic and early mitosis-arrested cells displayed negative TUNEL labeling (Figure 2a).

It is widely known that DNA fragmentation is a hallmark of apoptosis. This process is mediated by CAD after its inhibition is lifted by caspase cleavage of the inhibitor of CAD (ICAD).[31,32] This event contributes directly to the demise of the cell during apoptosis but is hardly reported in cells undergoing mitotic death. We postulated that the loss of chromosomal integrity during prolonged mitotic arrest might facilitate DNA fragmentation and drives cell death in mitosis.

Table 1 Table showing chromosomal length and width under different treatment

	HeLa		A549		Mcf-7	
	Length[a]	Width	Length	Width	Length	Width
Control	4.14 ± 1.37	0.7 ± 0.02	4.76 ± 1.43	0.66 ± 0.03	4.25 ± 1.24	0.63 ± 0.02
Taxol	2.9 ± 0.69	0.9 ± 0.06	2.56 ± 0.44	0.85 ± 0.04	4.2 ± 1.16	0.64 ± 0.02
Taxol+caspase inhibitor	4.1 ± 1.51	0.74 ± 0.04	N.A.	N.A.	N.A.	N.A.
Taxol+wild-type Cap-H	3.2 ± 0.72	0.96 ± 0.09	N.A.	N.A.	N.A.	N.A.
Taxol+Cap-H mutant	3.77 ± 1.12	0.75 ± 0.05	N.A.	N.A.	N.A.	N.A.
Vinblastine	3.28 ± 0.79	0.91 ± 0.03	3.11 ± 0.68	0.92 ± 0.03	N.A.	N.A.

Abbreviations: NA, non-applicable. [a]Length and width of chromosomes are measured in μm

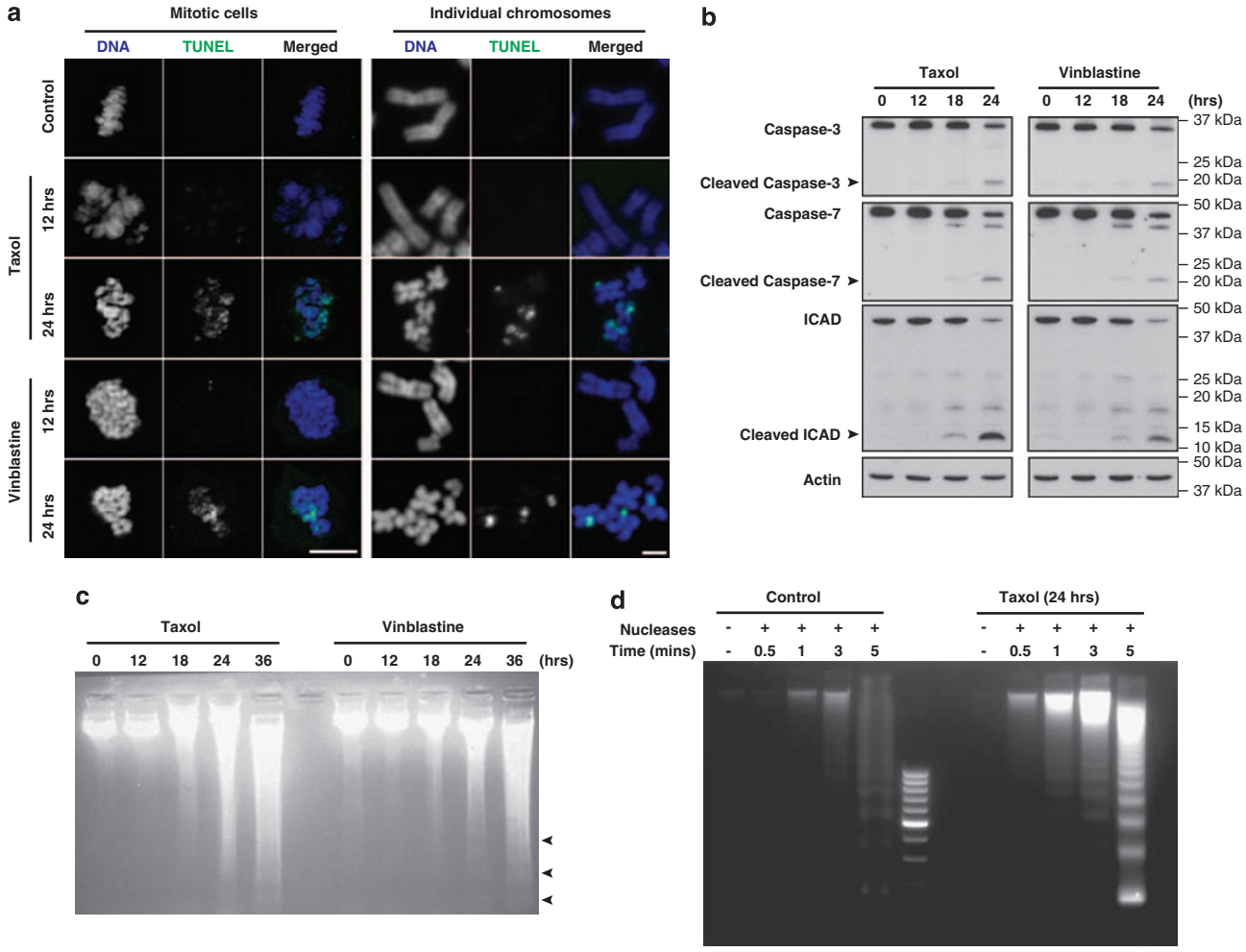

Figure 2 The loss of chromosomal integrity facilitates DNA fragmentation during mitotic death. (**a**) TUNEL assay showed presence of DNA damage on the chromosomes of prolonged mitosis-arrested cells treated with taxol or vinblastine. Mitotic cells: bar, 10 μm; individual chromosomes: bar, 2 μm. (**b**) Effector caspases-3, -7 and ICAD are cleaved after prolonged mitotic arrest. Actin served as a loading control. (**c**) Chromosomal DNA was collected from mitotic cells at various time points after drug treatment. The DNA was ethanol precipitated and analyzed on a 2% agarose gel. In all 10 μg of DNA was loaded in each well. Chromosomal DNA fragmentation occurred during prolonged mitotic arrest. Arrowheads indicate small DNA fragments. (**d**) In all 20 μg of chromosomal DNA from control and taxol-induced prolonged mitosis-arrested cells were subjected to fragmentation by excess amount of nucleases. No nucleases were added to the negative control. Only sheared DNA was collected and analyzed on a 2% agarose gel

Activated cleaved form of caspase-3 and -7 could be detected 18 h after drug treatment and the substrate of activated caspases, ICAD was also found cleaved (Figure 2b). To investigate the extent of DNA fragmentation in prolonged mitosis-arrested cells, chromosomal DNA was extracted from cells at various time points following taxol or vinblastine treatment and analyzed by agarose gel electrophoresis. DNA smears and smaller fragments of chromosomal DNA can be observed at 24 and 36 h post-treatment (Figure 2c). Thereafter, an *in-vitro* DNA fragmentation assay was performed to determine the susceptibility of the chromosomes to fragmentation by nucleases. Chromosomes were isolated from control mitotic cells and cells that have undergone a prolonged mitotic arrest induced by taxol. In all 20 μg of chromosomal DNA was subjected to digestion by an excess amount of nucleases at different time intervals and only sheared chromosomal DNA fraction was analyzed by agarose gel electrophoresis. DNA shearing of the aberrant chromosomes from prolonged mitosis-arrested cells was detected after a short incubation with the nucleases. An increased amount of sheared DNA with smaller-sized DNA fragments appeared at later time points, indicating more extensive shearing of the chromosomal DNA. In contrast, less sheared DNA was collected from the control mitotic chromosomes throughout the time course (Figure 2d). This indicates that chromosomes from prolonged mitosis-arrested cells were susceptible to DNA cleavage whereas chromosomes from control cells were more resistant. Taken together, these data show that DNA fragmentation occurs late during prolonged mitotic arrest and it is facilitated by the loss of chromosomal integrity.

Condensin I complex is absent from the chromosomes during prolonged mitotic arrest due to the degradation of Cap-H. Condensins, which are large pentameric complexes consisting of the core structural maintenance of chromosome-2 (SMC-2) and SMC-4 heterodimer plus three

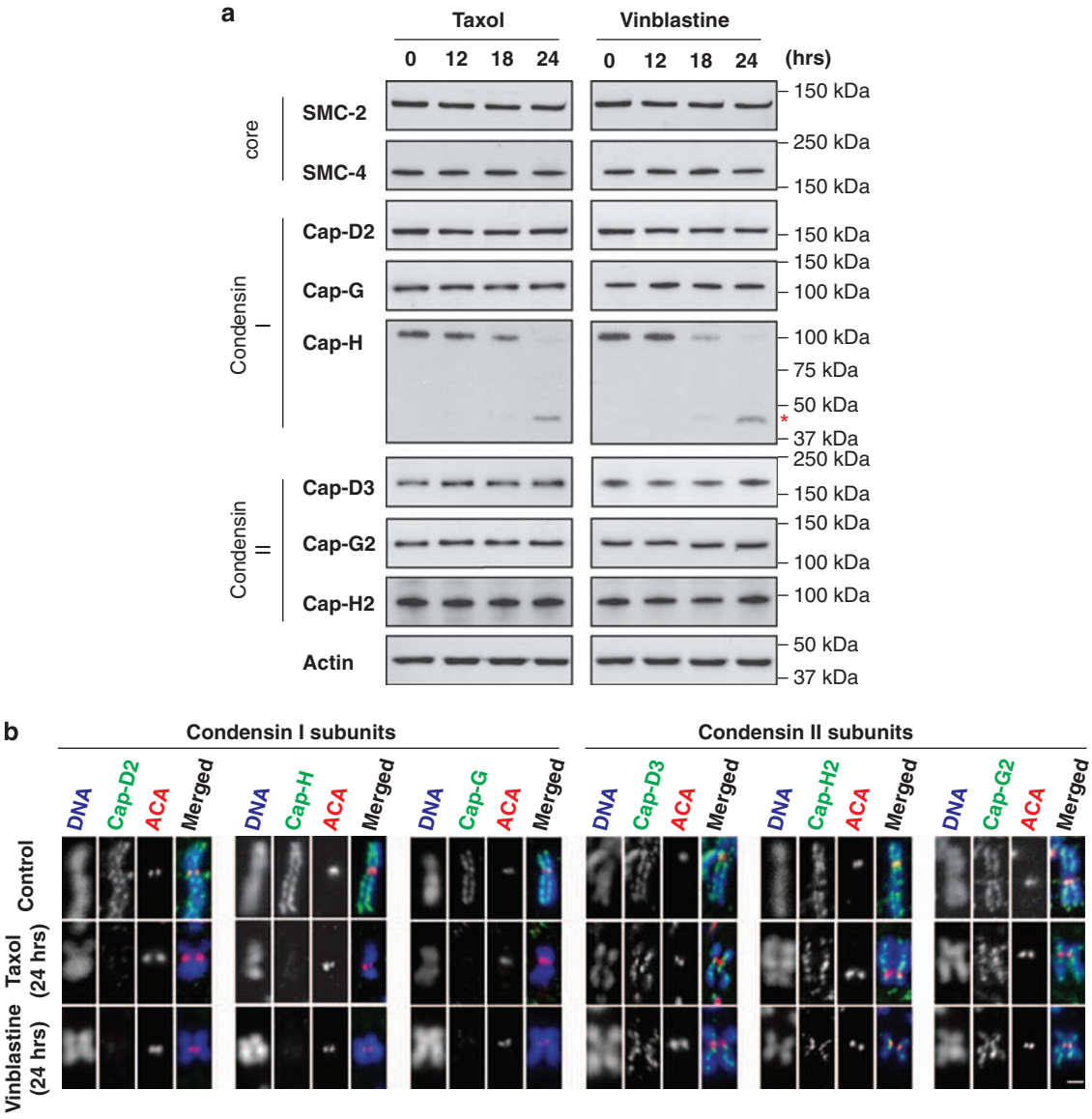

Figure 3 Cap-H is degraded during mitotic death and results in the loss of condensin I subunits on mitotic chromosomes. (**a**) Mitotic cells were obtained by mechanical shake-off at various time points after taxol or vinblastine addition. The cell lysates (25 μg) were separated on an 8% SDS-PAGE and the levels of condensin I and condensin II specific subunits were detected by western blot. Actin served as a loading control. The symbol '*' indicates cleaved form of Cap-H. (**b**) Immunofluorescence staining of condensin subunits on mitotic chromosomes. Condensin I subunits (Cap-D2, Cap-H and Cap-G) failed to localize along the chromosome axis in a defined pattern in prolonged mitosis-arrested cells induced by taxol and vinblastine. ACA is a centromeric marker. Bar, 1 μm

regulatory non-SMC subunits have important roles in regulating chromosome condensation, congression and maintenance of chromosomal integrity during mitosis.[33,34] Higher eukaryotes have two condensin complexes, condensin I and II. Both contain the same core heterodimer but differ in the regulatory subunits. Condensin I is composed of Cap-D2, Cap-H and Cap-G whereas condensin II contains Cap-D3, Cap-H2 and Cap-G2.[35] To determine if the changes observed in the chromosomal integrity during mitotic death were related to condensins, protein levels and cellular localization of all condensin subunits were probed. Mitosis-arrested cells were collected by mechanical shake-off at various time points after taxol or vinblastine treatment, followed by western blot. We observed a gradual decline in the level of Cap-H upon mitotic arrest and a gradual increase in a cleaved form of Cap-H. Other condensin subunits showed no significant changes in protein level (Figure 3a). In addition, immunofluorescence staining revealed the absence of condensin I subunits at the chromosomes during prolonged mitotic arrest. We concluded that the loss of Cap-H protein compromises the binding of other regulatory subunits of condensin I to the chromosomes. Localization of condensin II subunits on the chromosomes was unaffected during mitotic death (Figure 3b). Similar observations were also made for taxol-treated A549 cells (Supplementary Figure S2b). Hence, we propose that the alteration in

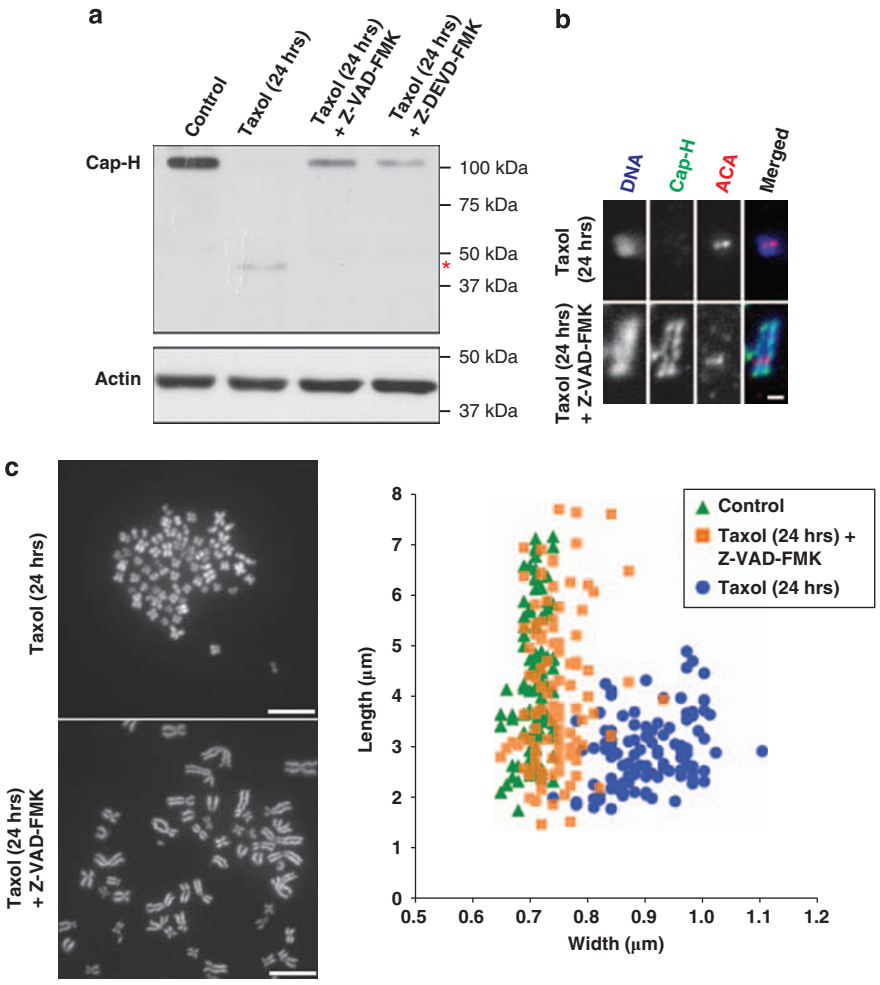

Figure 4 Depletion of Cap-H during mitotic death is correlated to caspase activity. (**a**) Presence of pancaspase inhibitor (Z-VAD-FMK) and caspase-3 inhibitor (Z-DEVD-FMK) prevented depletion of Cap-H during prolonged mitotic arrest. The symbol '*' indicates cleaved form of Cap-H. (**b**) Cap-H was able to localize onto chromosomes in the presence of pancaspase inhibitor. Bar, 1 μm. (**c**) Prolonged mitosis-arrested cells incubated in the presence of pancaspase inhibitor did not exhibit longitudinal shortening and widening of chromosomes. Differences in chromosome length and width between taxol + pancaspase inhibitor treated cells and control cells are statistically insignificant. Bar, 10 μm

chromosomal integrity during prolonged mitotic arrest was due to the loss of condensin I at the chromosomes as a result of Cap-H degradation.

Cap-H is a substrate of caspase-3 and its integrity regulates mitotic death. To check whether the decline in Cap-H level during mitotic death was correlated to caspase activity, pancaspase (Z-VAD-FMK) and caspase-3 (Z-DEVD-FMK) inhibitors were used to abrogate caspase activity. In the presence of these inhibitors, we were still able to detect Cap-H after a prolonged mitotic arrest induced by taxol, suggesting that Cap-H may be a substrate of caspases (Figure 4a). Furthermore, concomitant treatment of HeLa cells with taxol and pancaspase inhibitor did not cause any obvious change to the chromosome morphology and Cap-H remained localized on the chromosomes (Figure 4b and c). Hence, the degradation of Cap-H during prolonged mitotic arrest is most likely due to the activity of activated caspases.

Following that, we sought to identify potential caspase recognition sites in Cap-H in order to investigate if Cap-H is a direct substrate of caspases. It is known that executioner caspases preferentially recognizes a DXXD tetrapeptide motif and specifically cleaves after the aspartic acid residue at the fourth position.[36] Based on this convention, we identified seven potential cleavage sites on Cap-H and the aspartic acid residue was mutated to glutamic acid residue at each site (Figure 5a). The seven mutants (D357E, D360E, D363E, D366E, D374E, D377E and D380E) were fused to either an enhanced green fluorescent protein (EGFP) or a Flag tag to distinguish them from endogenous Cap-H. We evaluated each candidate site by an *in-vitro* caspase-3 assay. Flag-tagged Cap-H and the mutants were individually expressed in HEK cells, followed by immunoprecipitation and incubation with recombinant active caspase-3 for 0, 15 or 20 min. When the *in-vitro* assay products were analyzed by western blot, D363E and D366E mutants did not show any cleaved form of Cap-H. On the other hand, wild-type Cap-H and the rest of the mutants showed a gradual decline in the levels of full-length Cap-H in concomitant with the appearance of a lower-molecular-weight cleaved form (Figure 5a). It is therefore

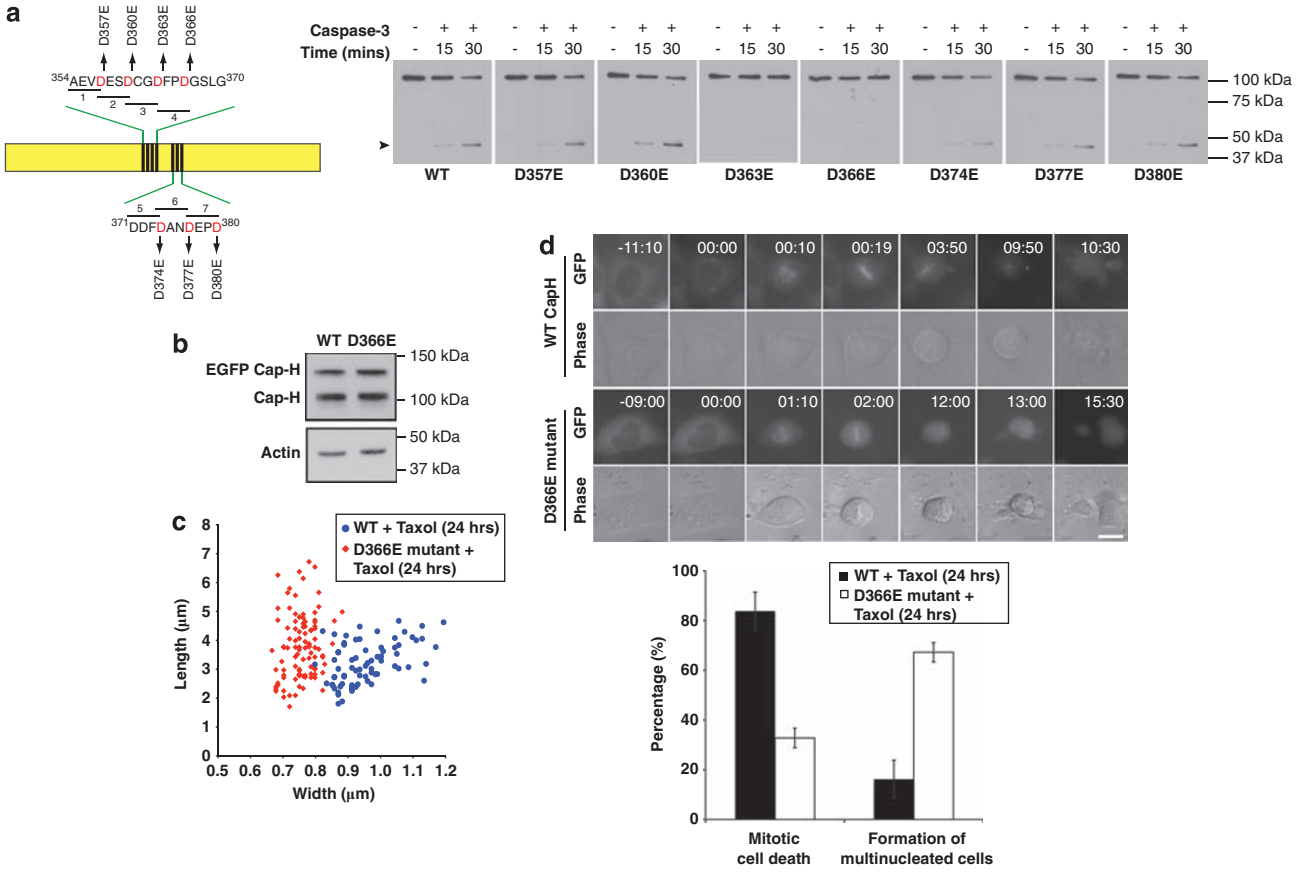

Figure 5 Cap-H is a substrate of caspase-3. (**a**) Schematic representation of Cap-H showing seven potential caspase recognition/cleavage sites. At each site, the aspartic acid residue (D) was mutated to a glutamic acid residue (E). The flag-tagged mutants were subjected to an *in-vitro* active caspase-3 assay. Arrowhead indicates cleaved form of Cap-H. No cleaved Cap-H band was observed for D363E and D366E mutant, indicating that caspase-3 recognizes the tetrapeptide sequence ^{363}DFPD^{366} and cleaves Cap-H after D^{366}. (**b**) Expression levels of EGFP-tagged wild type and D366E Cap-H proteins were similar in HeLa cells. (**c**) Chromosomes from prolonged mitosis-arrested cells expressing wild-type Cap-H have wider and shorter chromosomes as compared with cells expressing D366E mutant. Differences in chromosome length and width between these two samples are statistically significant at the $P<0.001$ level. (**d**) Majority of the cells expressing D366E mutant Cap-H were able to exit mitosis, whereas cells expressing wild-type Cap-H died in mitosis after a prolonged mitotic arrest induced by taxol. Fluorescence images were taken with the same exposure time. Values represent averages from three independent experiments (± S.D.)

possible that caspase-3 recognizes ^{360}DCGD^{363} or ^{363}DFPD^{366} and cleaves after D^{363} or D^{366}, respectively. Nonetheless, we concluded that cleavage at site D^{363} was less likely to occur because mutation at D^{360} of the tetrapeptide motif did not lead to rescue of Cap-H cleavage by active caspase-3. Instead, ^{363}DFPD^{366} should be the *bona fide* tetrapeptide motif and Cap-H cleavage occurs after D^{366} because mutation of the first and fourth aspartic acid of the motif prevented cleavage by active caspase-3.

We then expressed EGFP-tagged D366E Cap-H mutant and treated them with taxol to observe if there were any changes to the chromosome morphology and cell fate of the cells. The expression levels of both EGFP-tagged wild type and D366E Cap-H proteins were similar in HeLa cells (Figure 5b). Fluorescence-activated cell sorting (FACS) was done to obtain EGFP-positive cells. We observed that chromosomes from cells expressing wild-type Cap-H were on average shorter and wider than chromosomes from D366E mutant cells (Table 1, Figure 5c). Differences between the chromosome measurements of the two samples were statistically significant at the $P<0.001$ level. Furthermore, timelapse imaging revealed that 67% of the cells expressing EGFP-tagged D366E Cap-H were able to escape mitotic death and exit mitosis to form aneuploid cells. Conversely, only 16% of the cells expressing wild-type Cap-H were able to escape from the mitotic arrest. The remaining 84% of the cell population underwent mitotic death (Figure 5d). These results imply that the loss of Cap-H is important in driving cells towards mitotic death after a prolonged mitotic arrest. To further verify this, we used a breast carcinoma cell-line, Mcf-7, that does not express caspase-3[37] and subjected it to taxol treatment. We first confirmed the absence of caspase-3 in Mcf-7 cells by western blot. Next, we found that the depletion of Cap-H in HeLa cells under taxol treatment was abrogated in Mcf-7 cells. Cleavage of caspase-7 and ICAD during prolonged mitosis was unaffected in Mcf-7 cells (Supplementary Figure S3a). As expected, Cap-H was detected on the chromosome axis after prolonged mitotic arrest (Supplementary Figure S3b). Chromosome morphology was also unaffected. Measurements of the chromosome length and width were found to be statistically insignificant between control untreated and taxol-treated cells (Table 1,

Supplementary Figure S3c). More importantly, we found that majority of Mcf-7 cells did not die in mitosis. Instead, they managed to escape from mitotic arrest to form multinucleated cells (Supplementary Figure S3d).

Discussion

Mitotic death helps to maintain genomic integrity by eliminating cells undergoing defective mitosis. This cell death pathway is a common outcome in cancer cells that have been treated with chemotherapeutic drugs.[6,11,38] Despite its importance, the molecular mechanisms that regulate the execution of the mitotic death machinery remain ambiguous. It is clear that the drugs do not target the death mechanism directly. Instead, they cause a prolonged mitotic cell arrest that leads to accumulation of intracellular stresses and these factors may have a major role in the eventual demise of the cell.

A recent study has revealed that both caspase activation and the rate of cyclin B1 degradation influence the cell's decision to die in mitosis.[13,15] In addition, molecular factors such as the durability of the spindle assembly checkpoint,[18,38] p73-regulated activation of Bim[39] and unscheduled activation of cyclin-dependent kinase 1[40] have been reported to regulate mitotic death. Although these findings provide some insights on what cellular components are essential, they are insufficient to address the long-standing question of how prolonged mitotic arrest can lead to cell death.

Consistent with several reports, we show that cell death effectors such as caspases and CAD are activated during mitotic death (Figure 2b). More importantly, we are able to establish how these death effectors exert their function in a mitotic cell. During mitotic arrest, chromosomal DNA damage is observed.[27,28] It is hitherto unknown how DNA damage can occur on a highly condensed chromosome structure. Our study provides a detailed mechanism to explain how this process occurs and how it contributes to the demise of the cell in mitosis. We have observed alteration in chromosome morphology in prolonged mitosis-arrested cells. Furthermore, by using SEM to magnify the chromosomes up to 15 000 times, we are able to detect chromosomal surface abnormalities. The DNA is less tightly packed and loops were found protruding out from the chromosome surface (Supplementary Figure S1c). We proposed that the alteration in the chromosome structure creates accessible sites for activated CAD to cleave the DNA. This conclusion is supported by the data obtained from the *in-vitro* DNA fragmentation assay (Figure 2d). We demonstrated that intact chromosomes were more resistant to nucleases activity whereas chromosomes obtained from cells undergoing mitotic death were more susceptible to DNA cleavage. In addition, the change in chromosome structure is attributed to caspase-3-mediated degradation of Cap-H (Figure 3). Based on these data presented here, we propose that the DNA fragmentation in mitotic chromosomes, facilitated by the loss in chromosome integrity serves as a major death signal in mitosis-arrested cells.

Taken together, we have identified a novel molecular event that regulates mitotic death. Our model shows that caspase-3-mediated depletion of Cap-H is an important step of the mitotic

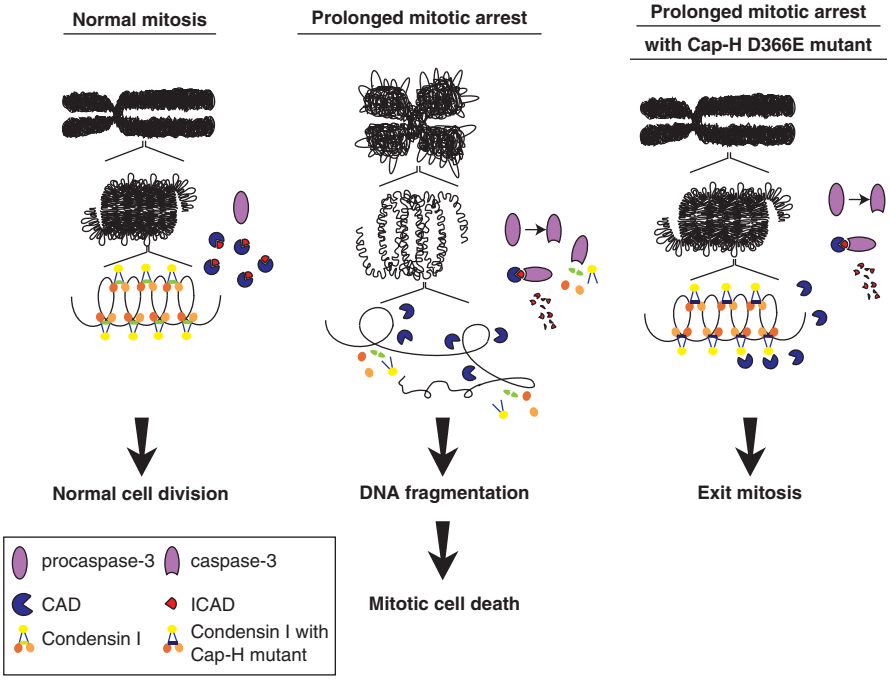

Figure 6 Model illustrating the link between caspase activation, chromosomal integrity and mitotic death. In normal mitotic cells, chromosomes are tightly condensed. Caspases are not activated and the cell proceeds through mitosis (left panel). In mitosis-arrested cells, caspase-3 is activated and cleaves a subunit of condensin I, Cap-H. This results in the loss of condensin I at the chromosomes and chromosomal integrity is altered. Subsequently, the chromosomal DNA is more susceptible to fragmentation by CAD and the cell dies during mitosis (middle panel). In the presence of a caspase-resistant form of Cap-H, the chromosomal integrity remains intact. This makes the DNA less accessible for fragmentation by CAD. The mitosis-arrested cells are more likely to exit mitosis to form aneuploid cells (right panel)

death process (Figure 6). Although the mitotic death pathway has been extensively described in the literature, to our knowledge, this is the first report to address how the mitotic death machinery is activated after a prolonged mitotic arrest. Our work here may have substantial implications in cancer therapy and drug development.

Materials and Methods

Cell culture, drug treatment and reagents. HeLa, Mcf-7, A549 and HEK cells were obtained from American Type Culture Collection and grown in Dulbecco's modified Eagle's medium (Gibco, Invitrogen, Carlsbad, CA, USA) containing 10% fetal bovine serum (Hyclone, Thermo Scientific, Logan, UT, USA) and 1% penicillin/streptomycin at 37°C in a humidified atmosphere with 5% carbon dioxide. For taxol and vinblastine treatment, 10 mg/ml of drug (Sigma-Aldrich, St. Louis, MO, USA) in dimethyl sulfoxide stock was diluted in medium to a final concentration of 10 nM. The caspase inhibitors z-DVED-FMK and z-VAD-FMK were from Calbiochem (La Jolla, CA, USA). Caspase inhibitors were used at a final concentration of 20 μM. Plasmids were transfected into HeLa cells using Lipofectamine 2000 reagent (Invitrogen, Carlsbad, CA, USA).

Chromosome spreads and SEM. Mitotic cells were collected by mechanical shake-off and incubated in hypotonic buffer (75 mM KCl) at 37°C. The cells were fixed with ice-cold fixative solution (methanol:acetic acid at 3 : 1). The fixed cells were dropped onto slides and stained with 4′,6-diamidino-2-phenylindole (DAPI; Invitrogen) the following day. The length and width of the chromosomes were measured using Axiovision 4.6 software (Carl Zeiss, Standort Gottingen, Vertrieb, Germany) and differences in measurements between samples were analyzed by the student *t*-test. For subsequent analysis by SEM, the chromosome spreads were fixed overnight with 2.5% glutaraldehyde in 0.1 M cacodylate buffer containing 0.1 M sucrose. After repeated washes with distilled water, the fixed chromosome spreads were subjected to alternating treatments with 1% osmium tetroxide (Sigma) and 0.5% thiocarbohydrazide (Sigma) until the chromosomes turned black. The spreads were then dehydrated with graded acetone solutions (25, 50, 75 and 100%). Images were acquired using an EVO LS 10 scanning electron microscope (Carl Zeiss).

FACS analyses. EGFP-positive cells were sorted in a flow cytometry cell sorter (FACSAria; BD Bioscience, San Jose, CA, USA) to separate them from non-transfected cells.

Immunofluorescence staining and microscopy. Cells were incubated in hypotonic buffer at 37°C for 30 min before centrifuging onto coverslips at 1000 r.p.m. for 5 min in a cytocentrifuge (Cytospin 2, Thermo/Shandon, Pittsburgh, PA, USA). The cells were permeabilized with 0.1% Triton X-100 in XBE2 (10 mM HEPES, pH 7.7, 2 mM $MgCl_2$, 100 mM KCl and 5 mM EGTA) at room temperature (RT) for 2 min and then fixed with 2% paraformaldehyde in XBE2 for 15 min. After several washes with phosphate buffered saline, cells were incubated with specific primary antibodies followed by fluorescent-labeled secondary antibodies and mounted onto glass slides using ProLong gold antifade reagent containing DAPI (Invitrogen). Images were acquired and analyzed using an Axiovert 200M inverted microscope (Carl Zeiss) and Axiovision 4.6 software.

Timelapse imaging. Cells were seeded onto 60 mm dishes and placed on a heat-controlled stage of a Zeiss Axiovert 200M microscope. The temperature was maintained at 37°C and CO_2 levels were maintained at 5% using a CTI 3700 controller (Carl Zeiss). Phase contrast and fluorescent images were recorded using the AxioCam camera and Axiovision 4.6 software.

Western blot. Mitotic cells were harvested by mechanical shake-off at various time points after taxol addition and lysed with M-Per mammalian protein extraction reagent (Pierce, Thermo Scientific-Pierce, Rockford, IL, USA) containing 10% complete EDTA-free protease inhibitor cocktail (Roche, Basel, Schweiz, Switzerland) and 0.1% phosphatase cocktail inhibitor 1 and 2 (Sigma). Equal amounts of protein were resolved by SDS-PAGE and transferred onto nitrocellulose membranes. The membranes were blocked with 5% skim milk in TBST (50 mM Tris, pH7.6, 150 mM NaCl, 0.1% Tween-20) for 1 h at RT and probed with specific primary and secondary antibodies. Signals were detected by an enhanced chemiluminescence reagent (Amersham Biosciences, Piscataway, NJ, USA).

DNA fragmentation assay. Mitotic cells collected by mechanical shake-off were lysed in 400 μl lysis buffer (200 mM Tris, 100 mM EDTA, 1% SDS) supplemented with 10 μl proteinase K (20 mg/ml). After incubation at 55°C for 3 h, 150 μl of saturated NaCl was added and subjected to centrifugation at 10 000 $\times$ *g* for 20 min. DNA was then ethanol precipitated and analyzed on a 2% agarose gel. In all 10 μg of DNA was loaded in each well.

***In-vitro* DNA fragmentation assay and TUNEL assay.** Mitotic cells collected by mechanical shake-off were lysed on ice in a buffer containing 10 mM HEPES (pH 7.9), 10 mM KCl, 1.5 mM $MgCl_2$, 0.34 M sucrose, 10% glycerol, 1 mM dithiothreitol, 0.25% Triton X-100 and a protease cocktail inhibitor (Roche). Cell lysates were passed through a 20-gauge needle at least 10 times. Chromosome fractions were collected by centrifugation at 1300 $\times$ *g* for 10 min. In all 20 μg of DNA was used for the assay. The chromosomes were sheared with 0.6U enzymatic shearing cocktail (Active Motif, Carlsbad, CA, USA) and incubated at 37°C at various time points. The reaction was stopped using ice-cold 0.5 M EDTA. Sheared chromosomes were collected by centrifugation at 15 000 $\times$ *g* for 10 min. Saturated NaCl was added to the supernatant and subjected to centrifugation at 10 000 $\times$ *g* for 20 min. The supernatant was mixed with ice-cold absolute ethanol and the mixture was centrifuged at 15 000 $\times$ *g* for 20 min. The pellet was then washed with ice-cold 70% ethanol and centrifuged at 15 000 $\times$ *g* for 5 min. The DNA pellet was allowed to air dry, resuspended in 20 μl RNase A solution and incubated at 37°C for 30 min. Fragmented DNA was analyzed on a 2% agarose gel. TUNEL assay was performed using the *in situ* cell detection kit (Roche).

Immunoprecipitation and active caspase-3 assay. Protein G-sepharose beads (Zymed, Carlton, CA, USA) conjugated to mouse anti-flag monoclonal antibody (Sigma) were incubated with cell lysates for 3 h at RT. The immunoprecipitates were washed with 150 mM NaCl in TBS and the beads were equally divided into three parts (60 μl each) for the active caspase-3 assay. The beads were first equilibrated in assay buffer (20 mM PIPES, 100 mM NaCl, 10 mM DTT, 1 mM EDTA, 0.1% (w/v) CHAPS, 10% sucrose, pH 7.2). Thereafter, the beads were spun down and 30 ng of active human caspase-3 (BD Pharmingen, San Jose, CA, USA) in assay buffer was added to each reaction and incubated at 37°C for 15 or 30 min. The reaction was stopped on ice and 5 $\times$ sample buffer was added, boiled at 100°C to denature the protein and separate it from the protein G beads. Products of the caspase-3 assay were analyzed by western blot using rabbit anti-flag polyclonal antibody.

Antibodies. The antibodies used were anti-actin goat polyclonal (Santa Cruz Biotechnology, Santa Cruz, CA, USA); anti-Cap-H rabbit polyclonal, anti-Cap-G rabbit polyclonal, anti-Cap-G2 rabbit polyclonal, anti-Cap-D2 rabbit polyclonal, anti-Cap-D3 rabbit polyclonal (Novus Biologicals, Littleton, CO, USA); anti-SMC-2 rabbit polyclonal, anti SMC-4 rabbit polyclonal (Abcam, Cambridge, UK); anti-Cap-H2 polyclonal antibody (Abgent, San Diego, CA, USA); anti DFF45 rabbit polyclonal (Abcam); anti-caspase -3 and -7 rabbit polyclonal (Cell Signaling Technology, Beverly, MA, USA); Alexa Fluor 488 goat anti-rabbit IgG, horseradish peroxidase-conjugated anti-mouse IgG, anti-rabbit IgG and anti-goat IgG (Invitrogen); and anti-flag rabbit polyclonal (Cell Signaling).

Conflict of interest

The authors declare no conflict of interest.

Acknowledgements. We thank Carl Zeiss Advanced Imaging Centre Singapore for technical assistance with scanning electron microscopy. This work was supported by Academic Research Council, Ministry of Education, Singapore (Academic Research Fund AcRF Tier 1, RG37/08) and A*STAR, Biomedical Research Council (BMRC grant 08/1/22/19/568).

1. Lowe SW, Lin AW. Apoptosis in cancer. *Carcinogenesis* 2000; **21**: 485–495.
2. Brown JM, Attardi LD. The role of apoptosis in cancer development and treatment response. *Nat Rev Cancer* 2005; **5**: 231–237.
3. Makin G, Hickman JA. Apoptosis and cancer chemotherapy. *Cell Tissue Res* 2000; **301**: 143–152.
4. Portugal J, Bataller M, Mansilla S. Cell death pathways in response to antitumor therapy. *Tumori* 2009; **95**: 409–421.
5. Roninson IB, Broude EV, Chang BD. If not apoptosis, then what? Treatment-induced senescence and mitotic catastrophe in tumor cells. *Drug Resist Updat* 2001; **4**: 303–313.

6. Mansilla S, Bataller M, Portugal J. Mitotic catastrophe as a consequence of chemotherapy. *Anticancer Agents Med Chem* 2006; **6**: 589–602.
7. Okada H, Mak TW. Pathways of apoptotic and non-apoptotic death in tumour cells. *Nat Rev Cancer* 2004; **4**: 592–603.
8. Schmidt M, Bastians H. Mitotic drug targets and the development of novel anti-mitotic anticancer drugs. *Drug Resist Updat* 2007; **10**: 162–181.
9. Sudakin V, Yen TJ. Targeting mitosis for anti-cancer therapy. *BioDrugs* 2007; **21**: 225–233.
10. Jackson JR, Patrick DR, Dar MM, Huang PS. Targeted anti-mitotic therapies: can we improve on tubulin agents? *Nat Rev Cancer* 2007; **7**: 107–117.
11. Weaver BA, Cleveland DW. Decoding the links between mitosis, cancer, and chemotherapy: the mitotic checkpoint, adaptation, and cell death. *Cancer Cell* 2005; **8**: 7–12.
12. Castedo M, Perfettini JL, Roumier T, Andreau K, Medema R, Kroemer G. Cell death by mitotic catastrophe: a molecular definition. *Oncogene* 2004; **23**: 2825–2837.
13. Gascoigne KE, Taylor SS. Cancer cells display profound intra- and interline variation following prolonged exposure to antimitotic drugs. *Cancer Cell* 2008; **14**: 111–122.
14. Gascoigne KE, Taylor SS. How do anti-mitotic drugs kill cancer cells? *J Cell Sci* 2009; **122**: 2579–2585.
15. Holland AJ, Cleveland DW. Beyond genetics: surprising determinants of cell fate in antitumor drugs. *Cancer Cell* 2008; **14**: 103–105.
16. Nunez G, Benedict MA, Hu Y, Inohara N. Caspases: the proteases of the apoptotic pathway. *Oncogene* 1998; **17**: 3237–3245.
17. Mansilla S, Priebe W, Portugal J. Mitotic catastrophe results in cell death by caspase-dependent and caspase-independent mechanisms. *Cell Cycle* 2006; **5**: 53–60.
18. Niikura Y, Dixit A, Scott R, Perkins G, Kitagawa K. BUB1 mediation of caspase-independent mitotic death determines cell fate. *J Cell Biol* 2007; **178**: 283–296.
19. Kitagawa K, Niikura Y. Caspase-independent mitotic death (CIMD). *Cell Cycle* 2008; **7**: 1001–1005.
20. Stevens JB, Liu G, Bremer SW, Ye KJ, Xu W, Xu J *et al.* Mitotic cell death by chromosome fragmentation. *Cancer Res* 2007; **67**: 7686–7694.
21. Brito DA, Rieder CL. The ability to survive mitosis in the presence of microtubule poisons differs significantly between human nontransformed (RPE-1) and cancer (U2OS, HeLa) cells. *Cell Motil Cytoskeleton* 2009; **66**: 437–447.
22. Shi J, Orth JD, Mitchison T. Cell type variation in responses to antimitotic drugs that target microtubules and kinesin-5. *Cancer Res* 2008; **68**: 3269–3276.
23. Jordan MA, Kamath K. How do microtubule-targeted drugs work? An overview. *Curr Cancer Drug Targets* 2007; **7**: 730–742.
24. Jordan MA, Wilson L. Microtubules as a target for anticancer drugs. *Nat Rev Cancer* 2004; **4**: 253–265.
25. Rieder CL, Maiato H. Stuck in division or passing through: what happens when cells cannot satisfy the spindle assembly checkpoint. *Dev Cell* 2004; **7**: 637–651.
26. Ha GH, Kim HS, Lee CG, Park HY, Kim EJ, Shin HJ *et al.* Mitotic catastrophe is the predominant response to histone acetyltransferase depletion. *Cell Death Differ* 2009; **16**: 483–497.
27. Dalton WB, Nandan MO, Moore RT, Yang VW. Human cancer cells commonly acquire DNA damage during mitotic arrest. *Cancer Res* 2007; **67**: 11487–11492.
28. Quignon F, Rozier L, Lachages AM, Bieth A, Simili M, Debatisse M *et al.* Sustained mitotic block elicits DNA breaks: one-step alteration of ploidy and chromosome integrity in mammalian cells. *Oncogene* 2007; **26**: 165–172.
29. Leslie M. Mitosis first, DNA repair later. *J Cell Bio* 2010; **190**: 160.
30. Giunta S, Belotserkovskaya R, Jackson SP. DNA damage signaling in response to double-strand breaks during mitosis. *J Cell Biol* **190**: 197–207.
31. Nagata S. Apoptotic DNA fragmentation. *Exp Cell Res* 2000; **256**: 12–18.
32. Sakahira H, Enari M, Nagata S. Cleavage of CAD inhibitor in CAD activation and DNA degradation during apoptosis. *Nature* 1998; **391**: 96–99.
33. Hudson DF, Vagnarelli P, Gassmann R, Earnshaw WC. Condensin is required for nonhistone protein assembly and structural integrity of vertebrate mitotic chromosomes. *Dev Cell* 2003; **5**: 323–336.
34. Hirano T. Condensins: organizing and segregating the genome. *Curr Biol* 2005; **15**: R265–R275.
35. Legagneux V, Cubizolles F, Watrin E. Multiple roles of condensins: a complex story. *Biol Cell* 2004; **96**: 201–213.
36. Degterev A, Boyce M, Yuan J. A decade of caspases. *Oncogene* 2003; **22**: 8543–8567.
37. Janicke RU. MCF-7 breast carcinoma cells do not express caspase-3. *Breast Cancer Res Treat* 2009; **117**: 219–221.
38. Vogel C, Hager C, Bastians H. Mechanisms of mitotic cell death induced by chemotherapy-mediated G2 checkpoint abrogation. *Cancer Res* 2007; **67**: 339–345.
39. Toh WH, Nam SY, Sabapathy K. An essential role for p73 in regulating mitotic cell death. *Cell Death Differ* 2009; **17**: 787–800.
40. Blank M, Lerenthal Y, Mittelman L, Shiloh Y. Condensin I recruitment and uneven chromatin condensation precede mitotic cell death in response to DNA damage. *J Cell Biol* 2006; **174**: 195–206.

Supplementary Information accompanies the paper on Cell Death and Differentiation website (http://www.nature.com/cdd)